

# SCAPE: Learning Stiffness Control from Augmented Position Control Experiences

Mincheol Kim, Scott Niekum, and Ashish D. Deshpande

**Abstract**—We introduce a sample-efficient method for learning state-dependent stiffness control policies for dexterous manipulation. The ability to control stiffness facilitates safe and reliable manipulation by providing compliance and robustness to uncertainties. So far, most current reinforcement learning approaches to achieve robotic manipulation have exclusively focused on position control, often due to the difficulty of learning high-dimensional stiffness control policies. This difficulty can be partially mitigated via policy guidance such as in imitation learning. However, expert stiffness control demonstrations are often expensive or infeasible to record. Therefore, we present an approach to learn Stiffness Control from Augmented Position control Experiences (SCAPE) that bypasses this difficulty by transforming position control demonstrations into approximate, suboptimal stiffness control demonstrations. Then, the suboptimality of the augmented demonstrations is addressed by using complementary techniques that help the agent safely learn from both the demonstrations and reinforcement learning. By using simulation tools and experiments on a robotic testbed, we show that the proposed approach efficiently learns safe manipulation policies and outperforms learned position control policies and several other baseline learning algorithms.

## I. INTRODUCTION

In recent years, deep reinforcement learning has been successfully used to improve object manipulation with robotic hands [1], [2]. However, one of the primary limitations of these works is that in most robotic hands, the robot joint poses are explicitly controlled and forces are implicitly decided. Such position control is cost-effective to implement, and results in fast, accurate position tracking. However, lack of explicit control over the force leads to limited safety and ability to handle uncertainties [3]. These might be critical factors when a robot is operating in an unstructured environments and during the exploratory phase of the learning process [4], [5].

Modulation of stiffness in concert with position control has been shown to address robustness, safety, and performance. Humans, for example, when faced with uncertainty, modulate stiffness by controlling muscle activations in response to afferent sensory signals [6]–[11]. Robots that collaborate in a human-friendly environment are often equipped with compliant mechanisms for improved robustness and safety [12], [13]. Similarly, stiffness control allows the robot to modulate its apparent compliance, thereby actively protecting the environment and itself [14].

Previous studies in manipulation with robotic hands have shown the potential of stiffness or force control for achieving dexterous manipulation [15]–[17]. However, stiffness control not only introduces hardware challenges, but it also imposes additional action dimensions, which affects sample-efficiency

of policy learning. This hindrance can be partially mitigated through guidance via imitation learning, providing the agent with a better starting point for reinforcement learning [18]. Expert demonstrations have been successfully collected and used in policy learning for position control-based robotic hands [1], [19], [20]. However, in the case of stiffness control, such expert demonstrations are expensive and difficult to acquire due to the necessity of specialized hardware for stiffness/force measurements and the ambiguity of expert behaviors.

A few attempts have been made to learn stiffness control policies. For example, a trajectory-centric strategy stabilizes around a given reference trajectory. A feedforward controller follows the trajectory as closely as possible, while the agent learns a feedback stiffness controller that compensates for the error [21]–[26]. While these methods work for simple periodic tasks where time-indexed stiffnesses suffice, they are unable to solve complex manipulation tasks that require a state-dependent controller where trajectories vary significantly. Other researchers have attempted to learn a state-dependent stiffness control policy from scratch [27]–[29]. This approach produces solutions for tasks that require versatility in initial and goal states, but learning from scratch is limited to low dimensional, simple tasks with short time horizons. In addition, due to the lack of policy guidance, increased dimensionality of the action space for stiffness often necessitates reward shaping that heavily depends on the task and the model [29].

In this paper, we present a novel learning strategy for a state-dependent stiffness control policy in a high-dimensional problem such as dexterous manipulation. Imitation learning is used within reinforcement learning to provide policy guidance, and we propose a way to bypass the need for stiffness demonstrations through an augmentation process. This process leverages the knowledge of the robot model such that we do not require actual stiffness control demonstrations but only position control. These position control demonstrations are augmented to infer approximate, suboptimal stiffness control demonstrations. To address this suboptimality, we use a Q-filter [19] to prevent the agent from mimicking dangerous choices that may appear in the inferred stiffness demonstrations. We also introduce the concept of an imitation regulator that controls the mode of imitation depending on the assessment of the current policy. Ablation studies show that these techniques play meaningful roles in both safety and stability of learning. We name our approach learning Stiffness Control from Augmented Position control Experiences (SCAPE).

Through simulation and experiments on a robotic testbed, we show that SCAPE produces a successful policy that is

robust to different types of uncertainties and safe in terms of force interaction. We include observation noise, random perturbations, and control failure during learning to simulate realistic environments. An episode is considered successful if the task is completed and the interaction between the robot and the environment meets the predefined safety requirements. Even under these challenging conditions, SCAPE results in strong policies that reach 100% success rates in the tested environments whereas existing position control approaches fail catastrophically.

## II. BACKGROUND AND RELATED WORKS

A majority of the past works in learning stiffness control rely on a reference trajectory which can either be fixed or generated from a pre-defined trajectory planner. In this paper we refer to these approaches as trajectory-dependent approaches. However, these approaches lack robustness to uncertainties, and variability in the task dynamics. Other recent research aims to learn a state-dependent stiffness controller that does not require additional trajectory planners, which we refer to as state-dependent approaches. In this section, we briefly explain some of the notable attempts to learn stiffness control, and discuss possible shortcomings.

### A. Trajectory-dependent Stiffness Controllers

The most common approach is to learn gain scheduling based on a given time-indexed trajectory and the deviation through  $PI^2$  [30], which is a trajectory optimization method based on a reference trajectory such that it can be tracked by the robot without modeling the inverse kinematics and dynamics. This approach added additional parameters to control compliance so that the resulting controller takes environment dynamics into account and modulates the gains accordingly [25], [26]. For example, by defining a time-indexed cost function for the  $PI^2$  algorithm, the robot learns to modulate the stiffness with respect to time. As a result, the robot successfully learns gain scheduling according to the learned dynamics of the environment, and still executes the planned trajectory. However, this approach does not account for force interaction and is purely driven by the kinematic error from the desired trajectory. Also,  $PI^2$  produces a feed-forward controller and cannot account for unforeseen disturbances or changes in the environment dynamics. Therefore, while it is suitable for repetitive tasks in a fixed environment with no regards for force interaction, it cannot be used for dexterous manipulation where it is crucial to generate vastly different trajectories depending on the current states and the goal.

Another approach uses an Incremental Gaussian Mixture Model (IGMM) and Gaussian Mixture Regression (GMR) to predict the interaction force for the next time-step, and feed-forward appropriate control effort [21], [22]. This method is inspired by the fact that humans tend to relax their muscles when they are comfortable completing the task, and that most of the generated motion is from a feed-forward controller based on predictions. If the robot detects a mismatch between

the predicted interaction force and the actual value, the feedback model increases the stiffness accordingly to correct the error in the trajectory. The goal of this approach is to learn a feed-forward model such that the feedback stiffness control effort can be minimized. However, this approach is also limited to a fixed trajectory that the robot learns initially, and the learned controller cannot cope with changes in environmental dynamics. Once the environment dynamics change, the IGMM needs to update its model iteratively to compensate for the difference. Therefore, this approach is limited to a fixed environment with a fixed desired trajectory, which is not ideal for dexterous manipulation.

Trajectory planners combined with reinforcement learning can also be used. Once the trajectory is defined, a residual control policy can be learned to adjust the gains according to the current observation. This method is mostly used in simple tasks where a trajectory planner is readily available, such as in peg-in-hole assembly tasks [23], [24]. In these works, the authors use reinforcement learning to produce a residual control policy on top of a hybrid force-position controller, where the corresponding gains are controlled by the policy. While this is a suitable approach for closed environments such as factories, it cannot be used for dexterous manipulation where desired trajectories can change according to the interacting forces. In addition, due to the lack of policy guidance, the learning process requires a complex reward function as well as an extensive amount of training time even with a trajectory planner aiding the policy search.

### B. State-dependent Stiffness Controllers

To account for a large degree of uncertainty in the environment, a learned stiffness controller must be state-dependent, instead of relying on a certain reference trajectory or gain scheduling that only works well in the training environment. Towards this goal, state-dependent stiffness control policies have recently been used and showed that learning variable impedance control is beneficial in contact sensitive tasks [27]. During hopping and wiping motions, the robots successfully produced better policies by employing joint-space stiffness control policies compared to direct torque control and position control policies. However, it is important to note that this approach is strictly limited to simple and repetitive low-dimensional movements. For instance, the robot was allowed to move only in one direction in the hopping task, and along a pre-defined circular path in the wiping task.

A similar work demonstrates the performance difference depending on the representation of the control policy [28], where the variable impedance control outperforms all the other representations in simple tasks. This approach aimed to complete kinematic tasks without any concern for force interaction. Despite the effort to simplify the problem into a lower-dimensional manifold by keeping the gripper closed in the door opening task, the variable impedance control approach failed to produce a better policy than a fixed impedance control approach. This is due to the curse of dimensionality that hinders policy search.

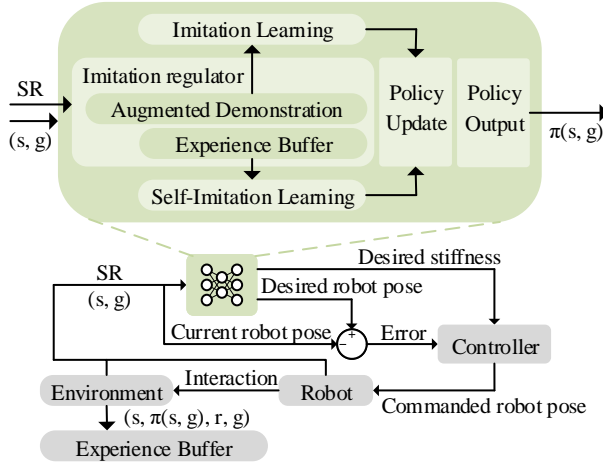


Fig. 1. Proposed learning scheme for SCAPE.

Another interesting work depicts the task-space impedance controller’s performance in quadruped locomotion [29]. The authors highlight the importance of the policy representation. Indeed, variable impedance control policies outperformed the direct torque control policy in terms of cumulative rewards and robustness to disturbances. Interestingly, both structured and highly structured policies resulted in more energy-efficient policies although the reward function did not consider energy. It is worth noting that an extensively tuned gait planner was provided to the agent to learn a successful policy.

While these state-dependent approaches show more promising results in terms of robustness to uncertainties, it is clear that such approaches are not well-suited for high-dimensional and long-horizon problems due to the lack of policy guidance.

### III. METHODS

In this section, we present our approach, SCAPE, to learn state-dependent stiffness control via imitation learning without requiring stiffness control demonstrations. Use of imitation learning within reinforcement learning improves policy guidance, thereby enabling high-dimensional dexterous manipulation [19]. We use Deep Deterministic Policy Gradient (DDPG, [31]), which is designed for continuous action spaces that are common in dexterous manipulation. We also employ Hindsight Experience Replay (HER, [32]) to further enhance sample-efficiency. HER uses Universal Value Function Approximators (UVFA, [33]) to imagine that some achieved state are as intended, allowing the agent to learn to generalize from failures and exploration. We use the same hyperparameters as OpenAI baselines [19], [34], except that the batch size remains 256. The overall learning scheme is depicted in Fig. 1, where the stiffness control policy takes in observed states  $s$  and the goal  $g$ , and produces an action  $\pi(s, g)$  which contains the desired stiffness in addition to the desired pose. Here, SR refers to the success rate of the current policy.

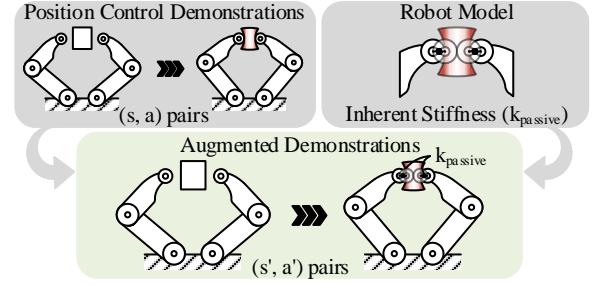


Fig. 2. Proposed augmentation process of position control demonstrations.

#### A. Demonstration Augmentation

A commonly used action representation in dexterous manipulation describes only the desired position of the actuator in the inner control loop, hence the name position control. This generates forces and torques that are induced by the inherent passive stiffness of the robot. On the other hand, a stiffness control policy outputs actions that describe the desired position of the actuators as well as the desired stiffness in the corresponding joint, as shown in Fig. 1.

However, as explained earlier, it is difficult to obtain expert stiffness control demonstrations for imitation learning. Therefore, we first bypass the requirement for stiffness control demonstrations through what we call an augmentation process shown in Fig. 2. More easily generated position control demonstrations are used, which complete the kinematic task but do not concern force interaction. We leverage the fact that the stiffness of the robot is known either from the simulation model or the hardware specifications, and that position control essentially works by moving to the desired position with the inherent stiffness or position gain of the actuator. In this paper, we refer to this inherent stiffness as  $k_{passive}$ . Therefore, state-action pairs,  $(s, a)$ , in common position control demonstrations can be augmented as that of stiffness control demonstrations,  $(s', a')$ , where the desired stiffness is  $k_{passive}$ . Consequently, these augmented demonstrations become suboptimal stiffness control demonstrations since the commanded stiffness of the robot is fixed to its passive stiffness  $k_{passive}$ , and force interaction was not considered during the demonstrations. We can then infer the reward function of the task from the augmented demonstrations, and use it to learn improved stiffness control.

#### B. Outperforming the Demonstration

Simple imitation learning in the form of reinforcement learning does not allow the agent to improve beyond the performance of the demonstrations due to the cloning loss [19]. The weight of the cloning loss can be decreased iteratively, assuming that the agent is able to learn a policy equivalent to the demonstrator early in the iteration [1]. But it is unclear how to determine the amount of dependency on the demonstrations with respect to the iteration. Also, simply reducing the dependency does not prevent the agent from cloning the undesirable behaviors seen in the suboptimal demonstrations we use. Therefore, we adopt additional tech-

niques to encourage the policy to outperform the augmented demonstrations and address its suboptimality.

1) *Q-Filter*: We use a Q-filter [19] to choose which replay transitions to clone from. The fundamental motivation behind learning from demonstrations is the assumption that the demonstrations provide a near-optimal action. However, this is not true for the augmented demonstrations. A Q-filter allows the agent to compare the Q values produced by the transitions from demonstrations,  $(s_i, a_i, g)$ , and the current policy,  $(s_i, \pi_\theta(s_i, g), g)$ . By comparing their values, the agent does not clone the behavior if its current policy provides a better action for the given demonstration state. More formally, the cloning loss  $L_{bc}$  can be defined as:

$$L_{bc} = \|a_i - \pi_\theta(s_i, g_i)\| \mathbb{1}_{Q(s_i, a_i, g_i) > Q(s_i, \pi_\theta(s_i, g_i), g_i)} \quad (1)$$

However, it is often difficult to infer the subtle difference in the qualities of the policies solely from examining the resulting Q estimates due to the overestimation issue of Q values [35]. Although the usage of the Q-filter improves the safety of learning, it tends to produce oscillatory gradients that prevent convergence of the policy due to its Boolean property [19].

2) *Imitation Regulator*: Therefore, we introduce an imitation regulator that observes the overall success rates of the current policy and determines the appropriate source of imitation from: 1) the augmented demonstrations and 2) the agent's own past experience. The latter is sometimes referred to as self-imitation learning [36]. The regulator controls the replay buffer  $\mathcal{D}_{IR}$  used for sampling transition batches to imitate as follows:

$$\mathcal{D}_{IR} = \begin{cases} \mathcal{D}_{demo}, & \text{if } SR < SR_{ref} \\ \mathcal{D}_{SIL}, & \text{otherwise} \end{cases} \quad (2)$$

where  $\mathcal{D}_{SIL}$  and  $\mathcal{D}_{demo}$  refer to the buffers that store the actual experience replay and the augmented demonstrations, respectively.  $SR \in [0, 1]$  is the overall success rate of the current policy and  $SR_{ref}$  is the reference success rate that is empirically found which is shown in Table I in Appendix A. Put simply, the regulator actively switches the source of demonstrations from  $\mathcal{D}_{demo}$  to  $\mathcal{D}_{SIL}$  once the success rate reaches  $SR_{ref}$ . This brings three primary benefits. First, the agent no longer references the suboptimal demonstrations which contains undesirable behaviors. Second, the policy can converge faster due to the minimized oscillation of gradients. Third, by cloning the previously generated actions, the agent can leverage exploration, thereby improving upon its current policy.

#### IV. ENVIRONMENTS

We use three robotic manipulation environments for simulation and experiments. For simulation, we use robots provided by OpenAI Gym [37], which uses the MuJoCo [38] physics engine. In all environments, we do not use the ground-truth force measurements during training. Instead, we use quasi-static force measurements from the series elasticity of the robot, which do not require force sensors. For safety

evaluation however, unless stated otherwise, we use ground-truth force measurements. A successful policy should meet both kinematic (e.g., did the object reach the goal states?) and safety (e.g., is the object intact?) goals. Furthermore, we implement a low-pass filter with a time constant of 0.05s for all force measurements in the simulation due to the low fidelity of the force tracking capabilities on MuJoCo. To validate the robustness under realistic conditions, we also include three types of uncertainties during training: 1) random perturbation to the object in a particular direction once it is within grasp, 2) measurement noise in the object's position, and 3) control failure that sometimes repeats the previous action.

##### A. Quasi-static Pick-and-place Environment (Block)

The Block environment shown in Fig. 3, entails a pick-and-place task with a parallel gripper. It is used to verify whether SCAPE is capable of learning a safe and robust manipulation policy under quasi-static assumptions. In this environment we assume that the force being exerted on the object comes entirely from the series elasticity of the gripper, which is reasonable to assume when the object is in grasp and the involved masses are small enough. Here, we made modifications to the existing *FetchPickAndPlace* environment on Gym to measure the interaction forces from series elasticity of a more compliant gripper. Also, the target location is always in the air to examine only the grasping solutions and discourage the use of other means of moving the object. All the changes made in the environment model are listed in Table II in Appendix A. In addition to the stiffness parameter,  $k_{lim}$  provides the upper limit for the stiffness controller. We found that having an extra parameter that controls the upper limit of the stiffness helps the policy converge faster to the minimum stiffness. Furthermore, such upper limit can be meaningfully related to the physical passivity of the robot [16].

Most importantly, the object is now considered broken if the interaction force exceeds a certain threshold called fragility shown in Table II. The goal in the original environment is to bring the object to the target location, and we call this a task-related kinematic goal that gives a reward of  $r_{task}(s) : s \rightarrow$

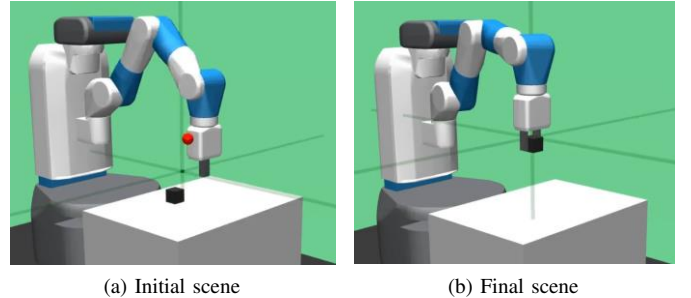


Fig. 3. Initial and final scenes of an episode for the Block environment are shown. The Block environment is a modified version of *FetchPickAndPlace* environment from Gym. The grippers are compliant and the object can now break. The observation space includes the positions of the object, gripper, and the goal in Cartesian space. The action space consists of Cartesian and open/close movements of the gripper, and the changes in the gripper stiffness and stiffness limit.

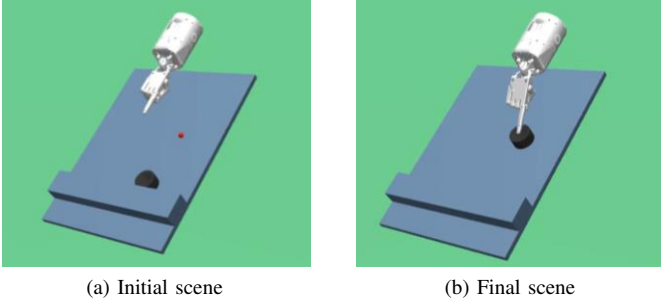


Fig. 4. Initial and final scenes of an episode for the Chip environment are shown. The hand has a compliant wrist and fixed finger joints. The observation space includes the positions of the object, fingertip, and the goal in Cartesian space. The fingertip velocity is also tracked in addition to the position. The action space consists of planar movement of the arm, the pitch movement at the wrist, and the changes in the wrist stiffness and stiffness limit.

$\{-1, 0\}$ . The Block environment requires an additional goal related to the safety of the surroundings: the object should never break throughout the episode. We aim to accomplish this goal by giving a safety-related reward of  $r_{safety}(s) : s \rightarrow (-\infty, 0]$ . Combining these reward functions naturally leads the agent to accomplish the kinematic goal while minimizing the estimated interaction force. Thus the overall reward function is defined as:

$$\begin{aligned} R(s) &= r_{task}(s) + r_{safety}(s) \\ r_{task}(s) &= \begin{cases} -1, & \text{if } \|\mathbf{x}_{o-g}\| > d \\ 0, & \text{otherwise} \end{cases} \\ r_{safety}(s) &= -\alpha \|\mathbf{F}\| \end{aligned} \quad (3)$$

where  $\mathbf{x}_{o-g}$  and  $\mathbf{F}$  are the relative position from the object to the goal, and the forces measured from series elasticity of each gripper. The distance threshold is  $d = 5\text{cm}$  and  $\alpha = 2e^{-3}$  normalizes the force. We use a sparse reward function for the task completion goal to avoid penalizing the agent from necessary exploration [32], and a dense reward function for the safety goal to minimize the interaction forces.

### B. Dynamic Pick-and-place Environment (Chip)

Chip environment in Fig. 4 is a dynamic version of the pick-and-place environment, designed to demonstrate that SCAPE produces a successful manipulation policy even in dynamic situations where the agent does not have access to ground-truth force measurements. It contains a Shadow hand, an object, and a slanted wall. The kinematic goal is to take the chip to the desired location by sliding it up the wall. The finger must not break the object, but at the same time, apply enough force so that it does not lose the object. In this case, the force being exerted on the object comes from not only the finger, but also from friction, which depends on velocity and normal force. The degree of freedom is kept minimal, allowing only planar movement for the arm parallel to the wall, and the wrist’s pitch movement that allows the finger to interact with the chip. The estimated interaction force is the wrist torque  $\tau$ , which is calculated from the series elasticity of the wrist actuator. Some of the important physical parameters of the environment are



Fig. 5. Initial and final scenes of an episode for the NuFingers environment are shown. NuFingers environment is a robot testbed to validate the practical efficacy of the proposed approach. The observation space includes the object and goal orientations as well as the positions and orientations of the fingertips. The action space consists of the radial movement that grasps object, the tangential movement that rotates the object, and changes in stiffness and stiffness limit.

shown in Table III in Appendix A. The only way to accomplish the kinematic goal is to utilize the friction between the finger and the object. Note that the agent does not have access to the ground truth force that the object experiences, which allows the extension of this work to practical applications where ground truth force measurements are unavailable. The reward function defined as:

$$\begin{aligned} R(s) &= r_{task}(s) + r_{safety}(s) \\ r_{task}(s) &= \begin{cases} -1, & \text{if } \|\mathbf{s}_{o-g}\| > d \\ 0, & \text{otherwise} \end{cases} \\ r_{safety}(s) &= -\alpha \|\mathbf{F}\| \end{aligned} \quad (4)$$

where  $\mathbf{s}_{o-g}$  is a state vector that contains the relative position from the object to goal as well as the velocity of the fingertip.  $\mathbf{F}$  is the wrist torque measured from series elasticity,  $d = 5\text{cm}$ , and  $\alpha = 2e^{-2}$ . Notice that the kinematic goal for the Chip environment includes a velocity goal. Without the velocity goal, the low fidelity of the friction in MuJoCo leads the agent to continuously move the object around the goal position without stopping. This phenomenon is likely due to the fact that the kinetic friction is usually smaller than the static friction. By adding the velocity goal, the agent is penalized from moving and thus able to successfully learn the task.

### C. In-hand Manipulation Environment (NuFingers)

To demonstrate the applicability for in-hand manipulation, we use the NuFingers testbed [16]. We first train the agent in a representative MuJoCo environment on Gym, and directly transfer the policy to the robot without any fine-tuning to validate the transferability and robustness of the resulting policies. The kinematic goal is to rotate the object to the desired orientation. The object has an integrated force sensor that directly measures the ground-truth force as well as an orientation sensor using a potentiometer. Also, elastic bands are installed that ground the object to the equilibrium orientation, providing resistance to the rotation. Similar to other environments, the ground-truth force measurements from the force sensor are not used during the training. Instead, we estimate the interaction forces from series elasticity of the



fingers. Observation and action spaces are depicted in Fig. 5. The reward function is defined as:

$$\begin{aligned} R(s) &= r_{task}(s) + r_{safety}(s) \\ r_{task}(s) &= \begin{cases} -1, & \text{if } \|\theta_{o-g}\| > d \\ 0, & \text{otherwise} \end{cases} \\ r_{safety}(s) &= -\alpha\|\mathbf{F}\| - \beta\|\dot{\mathbf{q}}\| \end{aligned} \quad (5)$$

where  $\theta_{o-g}$  is the difference between the goal and the current object orientation. The orientation error threshold is  $d = \frac{\pi}{16}$ . The vector  $\mathbf{F}$  contains the forces of each finger measured only in the grasping direction using series elasticity. The vector  $\dot{\mathbf{q}}$  contains joint velocities.  $\alpha = 4e^{-1}$ , and  $\beta = 1$  are normalization terms.

Furthermore, we apply domain randomization [2] during training to partially account for model discrepancies. We randomize the position and the width of the object, as well as the elasticity of the rubber bands of the object as shown in Table V in Appendix A. Note that other important dynamic properties such as backlash or Coulomb friction are not modeled in simulation even though they have considerable effects on the performance of the actual system.

## V. RESULTS

In this section, we demonstrate the performance of SCAPE in various environments. Without the proposed augmentation process, a stiffness control policy must be learned from scratch since stiffness control demonstrations are not available. However, the ablation study in Sec. V-B shows that learning stiffness control from scratch fails due to the lack of policy guidance. Therefore, we compare our results with position control where all the other conditions, such as a reward function and the application of the Q-filter or the imitation regulator, remain the same. This comparison demonstrates the importance of using state-dependent stiffness controllers as opposed to existing position controllers that are widely used in dexterous manipulation [1], [2].

### A. Experimental Results

Figure 6 depicts the success rates over epochs for the Block, Chip, and NuFingers environments. Solid lines refer to the mean values across the parallel rollouts and the shaded areas cover one standard deviation. For in-depth assessment, we break down the plots to also show success rates for the safety and kinematic goals. Safety-related success rates refer to the fraction of the time when the experienced force is smaller than the breaking threshold. For example, 0.9 means that the experienced force by the object exceeded the threshold 10% of the time during the episodes. Note that exceeding it at any time results in an overall failure in the corresponding episode. Task-related success rates only consider the kinematic goal which commonly used by the community.

Kinematic pick-and-place tasks without uncertainties have been easily solved by the position control policies in previous works [32]. However, Fig. 6a shows that position control policies fail to accomplish the overall goal which contains

both kinematic and safety goals. The heavy penalty from large forces discourages exploration and prevents the agent from learning to even grasp the object. SCAPE on the other hand, uses stiffness control policies to successfully minimize the interaction force and reaches a 100% success rate.

For the Chip environment where the action space is smaller, the position-controlled agent learns to complete the kinematic task entailed in the demonstrations to some degree as shown in Fig. 6b. However, it fails to address the safety issues, thereby breaking the object in almost all of the evaluation episodes. Note that unlike in the Block environment, the ground-truth force measurements are used for evaluation. It is significant that SCAPE still produced a successful policy by referencing only the quasi-static force measurements from the series elasticity, which do not include friction.

For the NuFingers environment in Fig. 6c, we find a similar trend as in the Block environment. The position control approach fails to learn a policy that completes the kinematic task. This failure is likely due to the heavy penalty from the interaction forces that prevent the agent from exploring further. SCAPE however, reaps the benefits of stiffness control and finds a successful policy. Most importantly, in spite of the model discrepancies between the simulation and the actual robot, the resulting policy proves to be successful after the sim-to-real transfer without additional training.

To summarize, it is evident that a state-dependent stiffness control policy outperforms the position control policy in terms of safety and robustness and that the proposed approach is capable of producing such policies.

Figure 7 depicts the force experienced by the object and the error for the kinematic goal after training for each environment. On the right, it also shows the progression of mean Q values, interaction forces, and stiffnesses throughout learning. It is evident that the proposed approach quickly learns to reduce the stiffness and settles at the necessary stiffness for the completion of the kinematic task. The stiffness and interaction force of the system are strongly related to one another as can be seen from the similar trends of the two curves. The existing approach which uses position control on the other hand, does not adjust the stiffness and therefore fails to reduce the interaction force.

Also, notice that the objects in the Chip and NuFingers environments experience much more force than what the robot can exert. This is because for evaluation, we use the ground truth forces which come from various sources, such as the friction that depends on the normal force and the velocity of the object. Also, we cannot ignore the poor force tracking in MuJoCo, which resulted in the spikes in Fig. 7c. The proposed approach, despite the lack of knowledge of the ground truth force, successfully minimizes it using only the practically available information.

### B. Safety and Ablation Study

Although it is evident that the proposed policy is successful in learning a safe policy under uncertainties, it is not yet clear whether the process of acquiring such policy is safe. In this

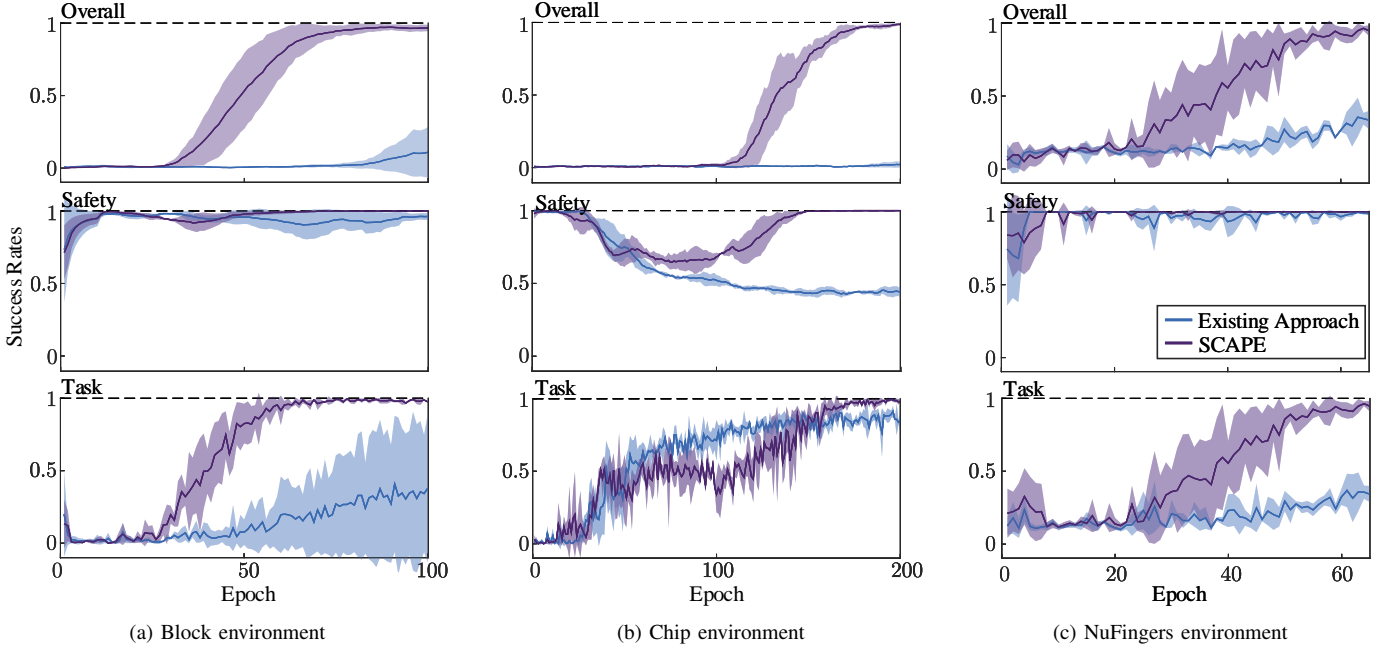


Fig. 6. Resulting success rates for the three environments. Success rates for task-related goals (e.g., did the object reach the target states?) and safety-related goals (e.g., how often did the object break?) are separately plotted. Overall goals entail both goals. Purple lines represent SCAPE with a state-dependent stiffness controller and blue lines represent the existing approach with a position controller.

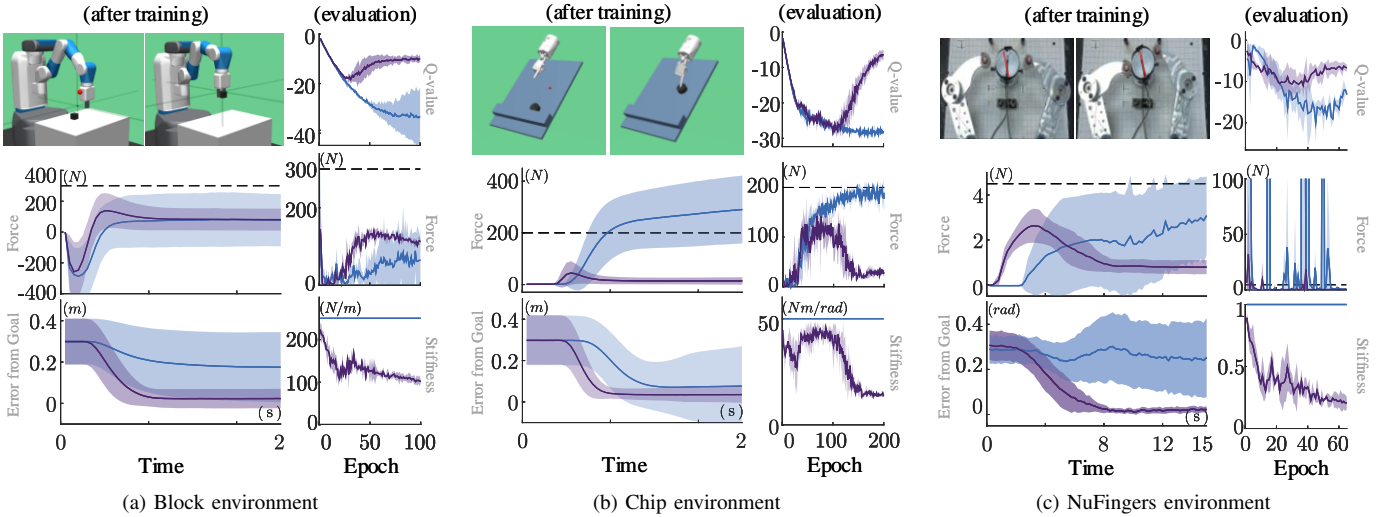


Fig. 7. For each of the environments, force experienced by the objects and kinematic error of the resulting policies are shown on the left. The mean Q values, forces, and stiffnesses evaluated in each epoch are shown on the right.

section we compare the safety of the different approaches during training and establish that SCAPE is safe and successful both during and after training. Furthermore, we identify the effects and roles of the various techniques used in SCAPE through an ablation study.

1) *Safety during Exploration*: To accurately examine the safety during the acquisition of successful policies, we measure the safety-related success rates during the exploration as shown in Fig. 6. Note that during exploration, we add Gaussian noise to the action to improve the policy. The corresponding success rates are shown in Fig. 8. Figure 8

shows a significant performance gap between SCAPE and position-controlled policies. SCAPE shows consistently safe performance throughout training, whereas almost half the time the position control policies apply greater force than what the object can withstand in either the beginning or ending phase of learning. Interestingly, these trends are similar to the evaluation results in 6. Note that the relatively high safety-related success rates of the position control for the Block and NuFingers environments are due to the failure in learning to manipulate the object, resulting in minimal interaction. From these results, we conclude that SCAPE is safer and superior

than the existing approach both during the exploration and after training.

2) *Ablation Study*: To examine the effects of each technique used in this paper, we approach the same learning problem defined by the Block environment under five different conditions:

- Condition 1: Reinforcement learning from scratch, without a Q-filter, without an imitation regulator
- Condition 2: Reinforcement learning + imitation learning from augmented demonstrations, without a Q-filter, without an imitation regulator
- Condition 3: Reinforcement learning + imitation learning from augmented demonstrations, without a Q-filter, with an imitation regulator
- Condition 4: Reinforcement learning + imitation learning from augmented demonstrations, with a Q-filter, without an imitation regulator
- Condition 5: Reinforcement learning + imitation learning from augmented demonstrations, with a Q-filter, with an imitation regulator

Condition 1 represents the approach taken by the researchers in the past [27]–[29], where imitation learning was not used due to the absence of demonstration data. Conditions 2-5 use the augmented demonstrations introduced in this paper, with different combinations of complementary techniques. Note that condition 5 is used to produce the results in Fig. 6.

Overall success rates generated under the different conditions are shown in Fig. 9. From these results, we confirm that learning from scratch does not produce any meaningful results for high dimensional and long-horizon problems (e.g., approaching an object, grabbing the object, and relocating the object). For this reason, the augmented demonstrations play a crucial role in providing guidance to the policy through imitation learning.

Moreover, in conditions 2 and 3, the agent is unable to filter out undesirable behaviors, thereby consistently breaking the object during exploration as shown in Fig. 10. Therefore, we confirm that the Q-filter allows the agent to make safe decisions by comparing the Q values of the demonstrated actions and the ones provided by the current policy. Also, applying the imitation regulator without the Q-filter fails from satisfying safety goals. Lastly, without the imitation regulator, the agent keeps referencing the suboptimal demonstrations even with the Q-filter, which causes oscillations and delays convergence. Instead, switching to self-imitation learning using the imitation regulator helps reinforce some of the past good behaviors preventing the policy from diverging, which is shown by the

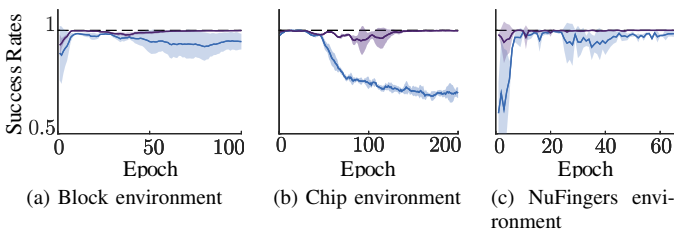


Fig. 8. Safety-related success rates for each environment during exploration.

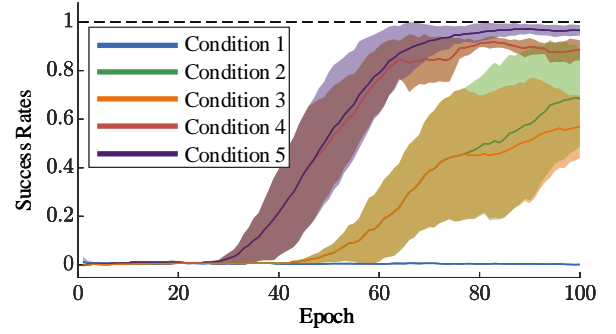


Fig. 9. Overall success rates for different conditions in the Block environment.

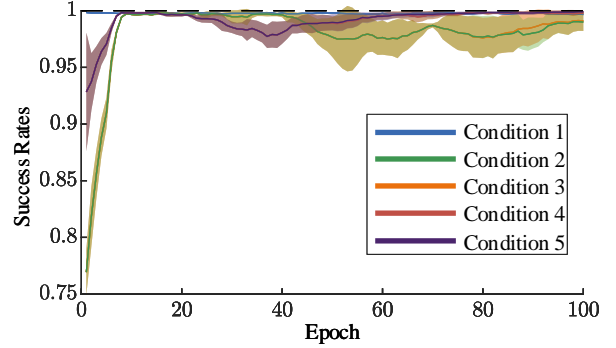


Fig. 10. Safety-related success rates during exploration. Conditions without the Q-filter blindly follows the suboptimal demonstrations thereby breaking the object continuously throughout learning.

higher mean and smaller variance of the condition 5 compared to those of condition 4.

## VI. CONCLUSIONS

We conclude that our approach, SCAPE, is capable of producing a successful state-dependent stiffness control policy, which plays a crucial role in ensuring safety and performance in dexterous manipulation. Most existing approaches for robotics manipulation only focus on kinematic goals so position control policies yield satisfactory results. However, in more realistic situations where robustness and safety are also critical, the state-dependent stiffness control policies vastly outperform the existing approaches. We observed that learning state-dependent stiffness control policies was challenging and the proposed process involving augmented demonstrations allowed the agent to overcome the sample-complexity and learn competent manipulation skills. Furthermore, the suboptimality of the augmented demonstrations was alleviated by a combination of the Q-filter and the imitation regulator, which resulted in faster and more stable convergence to a successful policy. Through the safety assessment during exploration, we also observed that SCAPE is consistently safer than using an existing position control approach. In the ablation study, the Q-filter and the imitation regulator were shown to prevent the agent from blindly imitating the suboptimal demonstrations, and to help focus on the past desirable experience. SCAPE ensures both safety and performance such that robust dexterous manipulation can be conveniently learned for real applications.



## REFERENCES

- [1] A. Rajeswaran, V. Kumar, A. Gupta, G. Vezzani, J. Schulman, E. Todorov, and S. Levine, "Learning complex dexterous manipulation with deep reinforcement learning and demonstrations." *arXiv preprint: 1709.10087*, 2017.
- [2] M. Andrychowicz, B. Baker, M. Chociej, R. Józefowicz, B. McGrew, J. Pachocki, A. Petron, M. Plappert, G. Powell, A. Ray, J. Schneider, S. Sidor, J. Tobin, P. Welinder, L. Weng, and W. Zaremba, "Learning dexterous in-hand manipulation." *The International Journal of Robotics Research*, pp. 3–20, 2020.
- [3] M. Li, H. Yin, K. Tahara, and A. Billard, "Learning object-level impedance control for robust grasping and dexterous manipulation." *IEEE International Conference on Robotics and Automation (ICRA)*, pp. 6784–6791, 2014.
- [4] T. Haarnoja, S. Ha, A. Zhou, J. Tan, G. Tucker, and S. Levine, "Learning to walk via deep reinforcement learning." *arXiv preprint: 1812.11103*, 2018.
- [5] B. Samuel, M. Taylor, and P. Stone, "Transfer learning for reinforcement learning on a physical robot." *Ninth International Conference on Autonomous Agents and Multiagent Systems-Adaptive Learning Agents Workshop (AAMAS-ALA)*, 2010.
- [6] F. Mussa-Ivaldi, N. H., and E. B., "Neural, mechanical, and geometric factors subserving arm posture in humans." *Journal of Neuroscience*, pp. 2732–2743, 1985.
- [7] A. Hajian and R. Howe, "Identification of the Mechanical Impedance at the Human Finger Tip." *ASME Journal of Biomechanical Engineering*, p. 109–114, 1997.
- [8] E. Burdet, R. Osu, D. Franklin, T. Milner, and M. Kawato, "The central nervous system stabilizes unstable dynamics by learning optimal impedance." *Nature*, pp. 446–449, 2001.
- [9] D. Franklin, E. Burdet, K. Tee, R. Osu, C. Chew, T. Milner, and M. Kawato, "CNS learns stable, accurate, and efficient movements using a simple algorithm." *Journal of Neuroscience*, pp. 11 165–11 173, 2008.
- [10] P. Haggard and J. R. Flanagan, "Hand and brain: the neurophysiology and psychology of hand movements," *Elsevier*, 1996.
- [11] N. Hogan, "Adaptive control of mechanical impedance by coactivation of antagonist muscles," *IEEE Transactions on automatic control*, pp. 681–690, 1984.
- [12] R. Deimel and O. Brock, "A novel type of compliant and underactuated robotic hand for dexterous grasping." *The International Journal of Robotics Research*, vol. 35, pp. 161–185, 2016.
- [13] J. Zhou, J. Yi, X. Chen, Z. Liu, and Z. Wang, "BCL-13: A 13-DOF Soft robotic hand for dexterous grasping and in-hand manipulation." *IEEE Robotics and Automation Letters*, vol. 3, pp. 3379–3386, 2018.
- [14] J. Salisbury, "Active stiffness control of a manipulator in cartesian coordinates." *19th IEEE conference on decision and control including the symposium on adaptive processes*, 1980.
- [15] T. D. Niehues, P. Rao, and A. D. Deshpande., "Compliance in parallel to actuators for improving stability of robotic hands during grasping and manipulation." *The International Journal of Robotics Research*, pp. 256–269, 2015.
- [16] M. Kim and A. Deshpande, "Balancing Stability and Stiffness Through the Optimization of Parallel Compliance: Using Coupled Tendon Routing." *IEEE Robotics & Automation Magazine*, 2021.
- [17] R. Mir, A. Marjaninejad, and F. J. Valero-Cuevas, "The utility of tactile force to autonomous learning of in-hand manipulation is task-dependent." *arXiv preprint: 2002.02418*, 2020.
- [18] S. Schaal, "Is imitation learning the route to humanoid robots?" *Trends in cognitive sciences*, pp. 233–242, 1999.
- [19] A. Nair, B. McGrew, M. Andrychowicz, W. Zaremba, and P. Abbeel, "Overcoming exploration in reinforcement learning with demonstrations," *IEEE International Conference on Robotics and Automation*, pp. 6292–6299, 2018.
- [20] H. Van Hoof, T. Hermans, G. Neumann, and J. Peters, "Learning robot in-hand manipulation with tactile features." *IEEE-RAS 15th International Conference on Humanoid Robots*, pp. 121–127, 2015.
- [21] M. Mathew, S. Sidhik, M. Sridharan, M. Azad, A. Hayashi, and J. Wyatt, "Online Learning of Feed-Forward Models for Task-Space Variable Impedance Control," *IEEE-RAS 19th International Conference on Humanoid Robots*, pp. 222–229, 2019.
- [22] S. Sidhik, M. Sridharan, and D. Ruiken, "Learning hybrid models for variable impedance control of changing-contact manipulation tasks." *The Eighth Annual Conference on Advances in Cognitive Systems*, 2020.
- [23] C. Beltran-Hernandez, D. Petit, I. Ramirez-Alpizar, T. Nishi, S. Kikuchi, T. Matsubara, and K. Harada, "Learning Force Control for Contact-rich Manipulation Tasks with Rigid Position-controlled Robots." *IEEE Robotics and Automation Letters*, pp. 5709–5716, 2020.
- [24] C. Beltran-Hernandez, D. Petit, I. Ramirez-Alpizar, and K. Harada, "Variable Compliance Control for Robotic Peg-In-Hole Assembly: A Deep-Reinforcement-Learning Approach." *Applied Sciences*, p. 6923, 2020.
- [25] J. Buchli, E. Theodorou, F. Stulp, and S. Schaal, "Variable impedance control a reinforcement learning approach," *Robotics: Science and Systems VI*, pp. 153–160, 2011.
- [26] E. Rombokas, M. Malhotra, E. Theodorou, E. Todorov, and Y. Matsuoaka, "Tendon-driven variable impedance control using reinforcement learning," *Robotics: Science and Systems VIII*, pp. 369–376, 2013.
- [27] M. Bogdanovic, M. Khadiv, and L. Righetti, "Learning variable impedance control for contact sensitive tasks." *IEEE Robotics and Automation Letters*, pp. 6129–6136, 2020.
- [28] R. Martín-Martín, M. A. Lee, R. Gardner, S. Savarese, J. Bohg, and A. Garg, "Variable impedance control in end-effector space: An action space for reinforcement learning in contact-rich tasks." *arXiv preprint: 1906.08880*, 2019.
- [29] K. Zhang, J. Lee, Z. Hou, C. de Silva, C. Fu, and N. Hogan, "How does the structure embedded in learning policy affect learning quadruped locomotion?" *arXiv preprint: 2008.12970*, 2020.
- [30] E. Theodorou, J. Buchli, and S. Schaal, "A generalized path integral control approach to reinforcement learning." *The Journal of Machine Learning Research*, pp. 3137–3181, 2010.
- [31] T. Lillicrap, J. Hunt, A. Pritzel, N. Heess, T. Erez, Y. Tassa, D. Silver, and D. Wierstra, "Continuous control with deep reinforcement learning." *arXiv preprint: 1509.02971*, 2015.
- [32] M. Andrychowicz, F. Wolski, A. Ray, J. Schneider, R. Fong, P. Welinder, B. McGrew, J. Tobin, O. Abbeel, and W. Zaremba, "Hindsight experience replay." *Advances in neural information processing systems*, pp. 5048–5058, 2017.
- [33] T. Schaul, D. Horgan, K. Gregor, and D. Silver, "Universal value function approximators," *International conference on machine learning*, pp. 1312–1320, 2015.
- [34] P. Dhariwal, C. Hesse, O. Klimov, A. Nichol, M. Plappert, A. Radford, J. Schulman, S. Sidor, Y. Wu, and P. Zhokhov, "Openai baselines," <https://github.com/openai/baselines>, 2017.
- [35] H. Van Hasselt, A. Guez, and D. Silver, "Deep reinforcement learning with double q-learning." *arXiv preprint: 1509.06461*, 2015.
- [36] J. Oh, Y. Guo, S. Singh, and H. Lee, "Self-imitation learning," *arXiv preprint: 1806.05635*, 2018.
- [37] G. Brockman, V. Cheung, L. Pettersson, J. Schneider, J. Schulman, J. Tang, and W. Zaremba, "OpenAI Gym," *arXiv preprint: 1606.01540*, 2016.
- [38] E. Todorov, T. Erez, and Y. Tassa, "Mujoco: A physics engine for model-based control." *IEEE/RSJ International Conference on Intelligent Robots and Systems*, pp. 5026–5033, 2012.

## APPENDIX A

TABLE I  
REFERENCE SUCCESS RATES FOR EACH ENVIRONMENT.

	Block	Chip	NuFingers
$SR_{ref}$	0.65	0.85	0.65

TABLE II  
LIST OF MODIFICATIONS TO MODEL PARAMETERS IN THE BLOCK ENVIRONMENT.

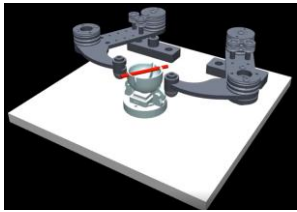
<i>Gripper Link</i>	Mass (kg)	Contact Dimension
Original	4	4
Modified	0.4	6
<i>Gripper Actuator</i>	Stiffness (N/m)	Control Range (m)
Original	30000	0.0 – 0.2
Modified	250	-1.0 – 1.0
<i>Gripper Joint</i>	Armature	Damping (Ns/m)
Original	100	1000
Modified	1	20
<i>Object</i>	Fragility (N)	Contact Dimension
Original	N/A	4
Modified	300	6

TABLE III  
LIST OF IMPORTANT MODEL PARAMETERS IN THE CHIP ENVIRONMENT.

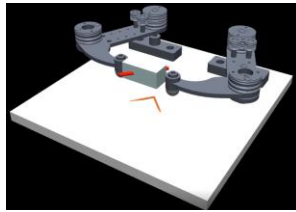
	Stiffness (N/m)	Control Range (m)
<i>Forearm Actuator (<math>x_1</math>)</i>	250	0.0 – 0.2
<i>Forearm Actuator (<math>x_2</math>)</i>	250	0.0 – 0.2
	Stiffness (Nm/rad)	Control Range (rad)
<i>Wrist Actuator</i>	50	-1.0 – 1.0
	Coefficients	Contact Dimension
<i>Friction<sub>finger-object</sub></i>	1	6
<i>Friction<sub>object-wall</sub></i>	1	3
	Fragility (N)	Mass (kg)
<i>Object</i>	200	0.1

TABLE IV  
LIST OF UNCERTAINTIES INCLUDED IN THE TRAINING AND EVALUATION.

Measurement Noise	
Property	Adds noise to the measurement <i>Uniform</i> (-1 cm, 1 cm) (Block, Chip) <i>Uniform</i> (-0.02 rad, 0.02 rad) (NuFingers)
Application	3D position of the object (Block, Chip) Rotation of the object (NuFingers)
Occurrence	100%
Random Perturbation	
Property	Adds velocity to the object <i>Uniform</i> (-50 cm/s, 50 cm/s) (Block, Chip) <i>Uniform</i> (-0.5 rad/s, 0.5 rad/s) (NuFingers)
Application	$x$ -dir (Block) $x_1$ -dir (Chip) $\theta$ -dir (NuFingers)
Occurrence	100%
Control Failure	
Property	Repeats the previous action
Application	Entire action
Occurrence	10%



(a) NuFingers Environment



(b) Approximated NuFingers Environment

Fig. 11. For stable contact between the surfaces in MuJoCo, the object in the NuFingers environment is approximated as a rotating block.

TABLE V  
LIST OF PARAMETER VARIATIONS FOR DOMAIN RANDOMIZATION IN THE NUFINGERS ENVIRONMENT.

Stiffness of Elastic Bands	
Variation	<i>Uniform</i> (0 N/m, 100 N/m)
Application	At the object base
Object Width	
Variation	<i>Uniform</i> (15 mm, 25 mm)
Application	Parallel to the grasping direction
Object Location on the Plane	
Variation	Original location + <i>Uniform</i> (-5 mm, 5 mm)
Application	Perpendicular to the grasping direction